

A Symbolic Approach to Detecting Hardware Trojans Triggered by Don't Care Transitions

Ruochen Dai
ruochendai@ufl.edu
ECE Department
University of Florida

Tuba Yavuz
tuba@ece.ufl.edu
ECE Department
University of Florida

Abstract

Due to the globalization of Integrated Circuit (IC) supply chain, hardware trojans and the attacks that can trigger them have become an important security issue. One type of hardware Trojans leverages the don't care transitions in Finite State Machines (FSMs) of hardware designs. In this paper, we present a symbolic approach to detecting don't care transitions and the hidden Trojans. Our detection approach works at both RTL and gate-level, does not require a golden design, and works in three stages. In the first stage, it explores the reachable states. In the second stage, it performs an approximate analysis to find the don't care transitions. In the third stage, it performs a state-space exploration from reachable states that have incoming don't care transitions to find behavioral discrepancies with respect to what has been observed in the first stage. We also present a pruning technique based on the reachability of FSM states. We present a methodology that leverages both RTL and gate-level for soundness and efficiency. Specifically, we show that don't care transitions must be detected at the gate-level, i.e., after synthesis has been performed, for soundness. However, under specific conditions, Trojan detection can be performed more efficiently at RTL. Evaluation of our approach on a set of benchmarks from OpenCores and TrustHub and using gate-level representation generated by two synthesis tools, Yosys and Synopsis Design Compiler (SDC), shows that our approach is both efficient (up to 10X speedup w.r.t. no pruning) and precise (0% false positives) in detecting don't care transitions and the Trojans that leverage them. Additionally, the total analysis time can achieve up to 3.40X (using Yosys) and 2.52X (SDC) speedup when synthesis preserves the FSM structure and the Trojan detection is performed at RTL.

1 Introduction

Globalization of the Integrated Circuit (IC) supply chain and the role of Third-party Intellectual Property (3PIP) in SoC development opened up possibilities for various attacks in the hardware domain. One type of attack is injecting malicious logic, which is called a hardware Trojan, into hardware designs or implementations. The Trojan is generally designed to be triggered on a certain input sequence or event to perform its malicious activity, which can be harming the circuit, changing the intended behavior, or leaking secret information.

Although the distributed nature of hardware development workflow is an important factor for this type of attack surface, the way a hardware component is designed and implemented can also have a role in the success of such attacks. An important type of vulnerability in hardware design is the don't care transitions in the Finite State Machines (FSMs). An FSM implements sequential control logic of a hardware component. When the transition function of an FSM is not defined

completely [3], there may exist some don't care transitions from some states. Although don't care transitions may provide opportunities for optimizing the synthesis, an attacker can exploit such transitions as a trigger mechanism for the malicious payload of a Trojan [3].

This paper presents a self-referencing (golden design free) Trojan detection at Register Transfer Level (RTL) as well as at gate-level and targets Trojans that are triggered by don't care transitions. These features make our approach applicable to four out of the seven types of attack models described in [27], in which the Third-party IP (3PIP) vendors, who typically deliver the IPs at RTL, are considered untrusted. These attack models consist of untrusted 3PIP vendor, commercial off-the-shelf component, untrusted design house, and fabless SoC design house.

The overall workflow of our approach is shown in the Figure 1 and leverages symbolic execution [9], a software testing technique that can potentially achieve high coverage of the system under analysis. We have implemented our approach on top of the KLEE symbolic execution engine [1]. We follow the approach in [32] and translate Verilog designs and their synthesized gate-level netlists into their C++ implementations using Verilator, which is a simulator for hardware designs [23]. So, we use the KLEE symbolic execution engine with don't care transition and Trojan detection extensions on the C++ implementations generated by Verilator.

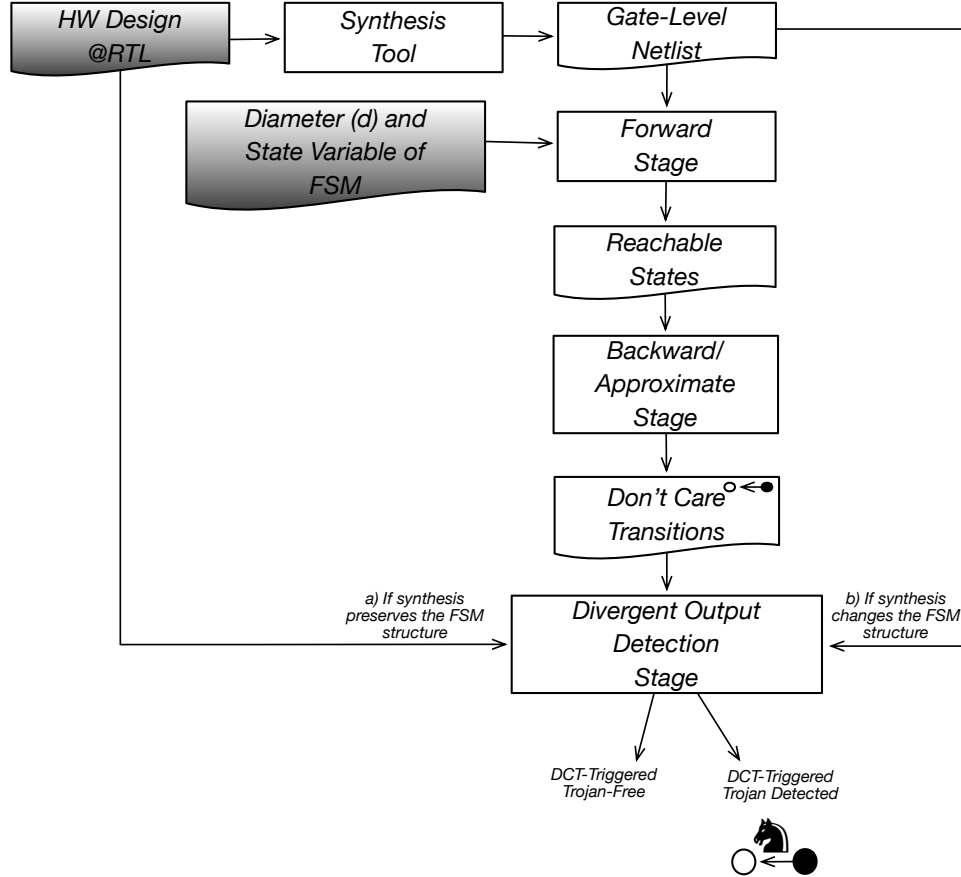


Figure 1: Overall workflow of the symbolic Trojan detection approach. Gray-filled boxes represent the inputs. Black-filled and white-filled circles represent the unreachable and reachable states of the FSM, respectively.

The presented approach works in three stages. In the first stage, we use symbolic execution to perform forward reachability analysis on the synthesized gate-level netlist up to a given number of clock cycles, which should be at least the diameter of the FSM under analysis. This stage is performed to compute the set of reachable states and input/output behavior while exercising all possible input sequences. In the second stage, we use an approximate analysis to find out the predecessors of reachable states. The goal of the second stage is to identify the don't care transitions by exercising all possible source states and inputs. This stage uses the reachable states computed in stage one to identify unreachable source states and reachable destination states.

The reason for performing the first and the second stages on the gate-level netlist instead of the RTL design is that the synthesis tools may introduce additional don't care transitions or change the FSM structure. Considering the fact that the Trojan attacks targeted in this paper would exploit the don't care transitions that exist in the synthesized circuit, this is important to achieve soundness for detecting Trojans that are triggered by don't care transitions.

Finally, in the third stage we perform another forward analysis up to a given number of clock cycles to detect any input-output behavior deviations for states that are reachable from states with incoming don't care transitions. So, our approach reports both the don't care transitions and the Trojans hidden at such transitions, if any, to help the designers harden their designs and evaluate the trustworthiness of 3PIPs. Our approach achieves optimized performance in two ways. The first one leverages a pruning approach that reduces the analyzed state space while guaranteeing sufficient coverage in inferring the set of reachable states. The second one leverages the structural properties of the synthesized FSM. If the synthesis tool preserves the FSM in terms of the states and the transitions between the states then the third stage can be performed at RTL. Our experiments show that this provides a more efficient detection while guaranteeing soundness. However, when the synthesis tool does not preserve the structure of the original FSM then the third stage must be performed at the synthesized gate-level netlist to achieve soundness with a performance cost.

Our tool will be publicly released along with the benchmarks from OpenCores [17] and those that were generated by adapting benchmarks from Trust-hub [22] and [25].

This paper is organized as follows. Section 2 places our work within the context of related work on finite state machine analysis and Trojan detection. Section 3 presents the technical details of our approach. Section 4 presents evaluation of our approach on various benchmarks. Section 5 discusses the limitations of our approach. Section 6 concludes with directions for future work.

2 Related Work

In this section, we discuss two groups of related work. The first group includes work that detect don't care transitions. The second group includes work that detect hardware Trojans.

Finite State Machine (FSM) Analysis The Netlist Analysis Toolset (NETA) [14] has been designed to help IP users extract FSMs from the low gate-level logic. However, this work does not identify any don't care transitions.

In [3], the authors consider don't care vulnerabilities in FSMs by using state reachability as a trust metric and by defining *incompletely specified FSMs* as those with unspecified next-states or output functions. Untrusted implementation of an FSM is detected by checking the existence of discrepancies between the original and the implemented FSMs in terms of the reachable states and the predecessors. The authors also discuss possible attacks that leverage the don't care transitions in unsafe implementations.

The AVFSM framework [15] extracts a state transition graph (STG) from a gate level netlist using an Automatic Test Pattern Generation (ATPG) approach. Don't care states and transitions are detected manually by comparing the extracted STG and the one that is generated from the RTL design by an EDA tool.

In [4], equivalence checking between an FSM specification and its gate level implementation is used to detect anomalies in the implementation. Both the specification and the implementation are represented as polynomials and symbolic algebra is used for equivalence checking.

Hardware Trojan Detection Various heuristics on how often Trojans get activated have been used to detect Trojans. These heuristic based approaches include identification of unused circuits [7], suspicious signals [33], suspicious wires [24], and dedicated triggers [31].

Formal verification approaches to Trojan detection require either functional specifications [19, 6] or security relevant specifications [13, 18].

Self-referencing techniques [16, 34, 11, 30, 8, 28, 29], which eliminate the need for a golden chip, leverage various physical characteristics of the circuits to detect Trojans during post-silicon analysis.

Dangerous don't care signals are detected in [5] by checking existence of distinguishing input sets that yield different observable output values. The analysis performs combinational equivalence checking on the attacker observable outputs between two copies of the same RTL design that differ only in the assignments of the don't care signals.

To our knowledge, our don't care transition identification and Trojan detection approach is the first self-referencing technique at RTL as well as at gate-level, thanks to leveraging an approximate symbolic exploration of the state space. Although our approach focuses on the don't care transition triggered Trojans, unlike the heuristic based approaches [7, 33, 24, 31], it does not rely on implementation details. Also, unlike the formal verification based approaches, our approach does not require any specifications. Finally, unlike [5], our approach considers sequential semantics as it computes the set of reachable states.

3 Approach

In this section, we present the technical details of our approach for detecting Trojans hidden at don't care transitions. Section 3.1 presents some fundamental notations about Finite State Machines (FSMs) with inputs and outputs along with some observations that we leverage in our detection approaches. Section 3.2 presents our two-staged approach for don't care transition detection and discusses various symbolic exploration approaches. Section 3.3 presents our three-staged approach for detecting Trojans hidden at don't care transitions and explains how symbolic execution is utilized in all the three stages.

3.1 Preliminaries

Definition 1 (Mealy Machine). A Mealy machine M is a 6-tuple $(S, S_0, \Sigma, \Lambda, T, G)$, where S is the set of states, S_0 is the set of initial states, Σ and Λ are the sets of input and output alphabets, respectively, $T : S \times \Sigma \rightarrow S$ is a transition function, and $G : S \times \Sigma \rightarrow \Lambda$ is an output function.

Definition 2 (Reachability). A state $s \in S$ is reachable in M if either s is in S_0 or there exists a sequence of inputs i_1, \dots, i_k such that starting from some initial state $s_0 \in S_0$, a sequence of transitions visit s_0, s_1, \dots, s_k , where $s_k = s$, according to the transition function T , i.e., $\exists k >$

0. $\exists s_0 \in S_0. \exists i_1, i_2, \dots, i_k. s_k = s \wedge \forall 0 \leq j < k. T(s_j, i_{j+1}) = s_{j+1}$. A state s is unreachable if it is not reachable.

Definition 3 (Bounded Reachability). Let $R(M)$ denote the reachable states in M . For a given integer $j \geq 0$, $R(M)_j$ denotes the set of reachable states that are reachable in at most j steps. $R(M)_0 = S_0$, and there exists $j \geq 1$ and $s_0 \in S_0, s \in R(M)_j \leftrightarrow (s \in R(M)_{j-1} \vee \exists i_1, i_2, \dots, i_j. \forall 0 \leq k < j. T(s_k, i_{k+1}) = s_{k+1} \wedge s_j = s)$.

Definition 4 (Diameter and Rank). The maximum distance of a state s in M is the longest Hamiltonian path from some initial state in S_0 to s . The diameter of M , $D(M)$, is the largest maximum distance among all the reachable states in M . For a given reachable state s in M , the rank of s is defined as the smallest j such that $s \in R(M)_j$.

Definition 5 (Cut). Let $M^{S'}$ denote a cut of $M = (S, S_0, \Sigma, \Lambda, T, G)$ with respect to a set of initial states S' , i.e., $M^{S'} = (S, S', \Sigma, \Lambda, T, G)$, where $S' \subseteq S$.

Claim 1 (Monotonicity of Bounded Cut Reachability). Given a Mealy Machine M and a state s that is reachable in M , the set of reachable states from s does not shrink with increasing values of bounds, i.e., $\forall j.k. 0 \leq k < j. R(M^{\{s\}})_k \subseteq R(M^{\{s\}})_j$.

Proof. Follows from the monotonicity of the successor function. \square

Algorithm 1: Computing the set of don't-care transitions in a Mealy Machine M .

Input: $M = (S, S_0, \Sigma, \Lambda, T, G)$: Mealy Machine, d : Diameter

Output: Set of don't care transitions

```

1  $s_0 \leftarrow \text{init}(P)$ ;
2  $RS \leftarrow \{s_0\}$ ;
3 for  $i$ : 1 to  $d$  do
4    $RS \leftarrow RS \cup \{s' \mid s \in RS \wedge \exists I. T(s, I) = s'\}$ 
5 end
6  $Trans \leftarrow \{(s_1, s_2) \mid s_2 \in RS \wedge \exists I. T(s_1, I) = s_2\}$ ;
7  $DCT \leftarrow \{(s_1, s_2) \mid s_1 \notin RS \wedge (s_1, s_2) \in Trans\}$ ;
8 return  $DCT$ ;
```

Definition 6 (Input Partition). Let $M_I = (S, S_0, \Sigma, \Lambda, T', G')$ denote the partitioning of M with respect to a sequence of input sets $I = I_1, I_2, \dots, I_k$, where k is at most $D(M)$, $\forall 1 \leq j \leq k. I_j \subseteq \Sigma$, and

$$\begin{aligned}
& s_0 \in S_0 \wedge \forall 1 \leq j \leq k. \\
& ((i_j \in I_j \wedge T(s_{j-1}, i_j) = s_j \wedge G(s_{j-1}, i_j) = o_j) \leftrightarrow (T'(s_{j-1}, i_j) = s_j \wedge G'(s_{j-1}, i_j) = o_j)) \wedge \\
& (i_j \notin I_j \leftrightarrow (T'(s_{j-1}, i_j) = \text{undef} \wedge G'(s_{j-1}, i_j) = \text{undef}))
\end{aligned} \tag{1}$$

Claim 2. The set of reachable states in a partition of M with respect to I is a subset of or equal to the set of reachable states in M , i.e., $R(M_I) \subseteq R(M)$.

Proof. Follows from the fact that the initial states of M_I is the same as the initial states of M and that the transitions in M_I is a subset of the transitions in M . \square

Definition 7 (Predecessors). The set of predecessors of state s for input i , $Pred(s, i)$, in M is the set of predecessor states that can reach s in one step on input i , i.e., $Pred(s, i) = \{s' \mid \exists s' \in S. T(s', i) = s\}$.

Definition 8 (Don't Care Transition). A don't care transition from s' to s on input i in M exists if s' is unreachable in M , s is reachable in M , and there is a transition from s' to s , i.e., $s' \notin R(M) \wedge s \in R(M) \wedge T(s', i) = s$.

```

1  always @ (posedge clock or posedge reset)
2  begin
3      if (reset) ..
4      else
5      begin
6          case (pcmSq) // waiting for a new input sample
7              'IDLE:
8                  if (inValid)
9                      begin
10                         ...
11                         pcmSq <= 'SIGN;
12                     end
13                  else ...
14              'SIGN:// check the difference sign and
15                  // set PCM sign bit accordingly
16              begin
17                  ...
18                  pcmSq <= 'BIT2;
19              end
20              'BIT2:
21              begin
22                  ...
23                  pcmSq <= 'BIT1;
24              end
25              'BIT1:
26              begin
27                  ...
28                  pcmSq <= 'BIT0;
29              end
30              'BIT0:
31              begin
32                  ...
33                  pcmSq <= 'DONE;
34              end
35              'DONE:
36              begin
37                  ...
38                  pcmSq <= 'IDLE;
39              end
40              // unused states
41              default:      pcmSq <= 'IDLE;
42          endcase
43      end
44  end

```

Figure 2: A snippet of the Verilog implementation of the FSM in the IMA ADPCM benchmark.

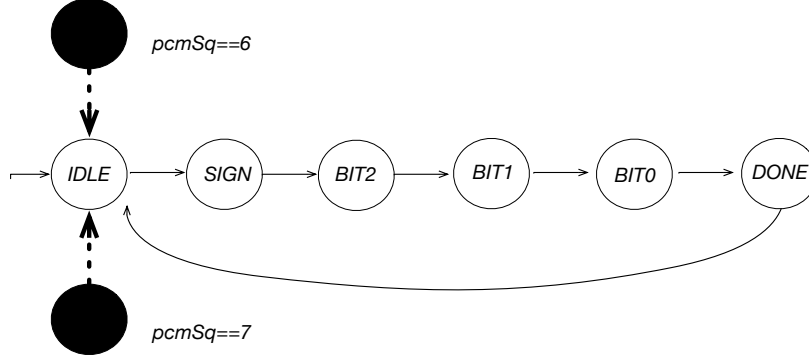


Figure 3: The FSM that corresponds to the RTL design in Figure 2. White-filled and black-filled circles represent the reachable and unreachable states, respectively. Dashed lines represent don't care transitions.

Figure 2 shows a snippet of Verilog code for the FSM part of one of our benchmarks, IMA ADPCM, which implements an audio compression algorithm [25]. The `pcmSq` register stores the FSM state and it is three bits wide. However, only values 0-5 are reachable states as the lines 11, 18, 23, 28, 33, and 38 indicate. The `default` case at line 41 allows transitioning from unreachable states, with values 6 and 7, to one of the reachable states, ‘PCM_IDLE, which is defined as 0. The FSM with reachable and unreachable states and the don't care transitions of this design are depicted in Figure 3. Such unreachable states can be realized through a physical attack and by exploiting don't care transitions that take the FSM from unreachable states to reachable ones, the attacker can violate safety and security properties.

3.2 Detecting Don't Care Transitions

In this section, we first introduce our approach at a high-level in Section 3.2.1. We briefly introduce a background on Symbolic Execution in Section 3.2.2. We discuss detecting don't care transitions using symbolic execution in Section 3.2.3.

3.2.1 High-level Approach

We assume that the diameter of the Mealy Machine M under analysis is known and denoted by d . Figure 4 shows our two stage approach. The first stage consists of a forward analysis, which computes the set of reachable states in d steps. The second stage uses a backward analysis, which compute the predecessors of every state in M . Algorithm 1 shows the high-level algorithm of our approach.

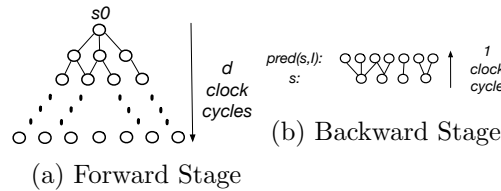


Figure 4: Two stages of don't care transition detection.

3.2.2 Background on Dynamic Symbolic Execution

Dynamic symbolic execution is a static program analysis technique that can reason about symbolic inputs. The word “dynamic” refers to the fact that concrete and symbolic values can be mixed on an execution path [2]. Dynamic symbolic execution has two major flavors: concolic and execution-tree generation based. A symbolic execution engine typically interprets the instructions of an intermediate language, such as the LLVM IR [12, 10], so that expressions that involve symbolic values are manipulated according to the semantics of the instruction. In this paper, we focus on the execution-tree generation based approach. When interpreting conditional branch instructions with symbolic branch conditions, a symbolic execution engine checks the satisfiability of the branch condition for each target using an SMT solver and to simulate each feasible target it generates a separate path. On each path it conjoins the symbolic branch conditions to generate the *path constraint*. So, the symbolic execution engine generates a tree of symbolic execution paths or states, where the internal nodes with multiple children denote branching points and each leaf node denotes a completed execution corresponding to an equivalence class of the input space. A challenge in symbolic execution is the well-known path explosion problem as the tree of executions may grow exponentially with the increasing number of branching instructions. So, symbolic execution is typically configured to run up to some timeout value.

3.2.3 Finding Don’t Cares Using Symbolic Execution

In this section, we explain how we use symbolic execution to perform the two-stage analysis that we present in Figure 4 and Algorithm 1. We have implemented our approach on top of the KLEE symbolic execution engine. We have used Verilator to translate the RTL design as well as the synthesized gate-level netlist into C++, and we used the clang compiler to generate the LLVM bitcode from the C++ code. One of the strengths of symbolic execution is the ability to explore the input space in a systematic way.

In the forward stage, we label the input variables, e.g., `inValid` in Figure 2, as symbolic in each of the d number of steps. This makes sure that each step gets a fresh symbolic variable and that the input values for each step are independent. Therefore, all sequences of input equivalence classes are explored within a time bound. We record the FSM state reached in each symbolic execution state in a global metadata structure that represents the set of reachable states.

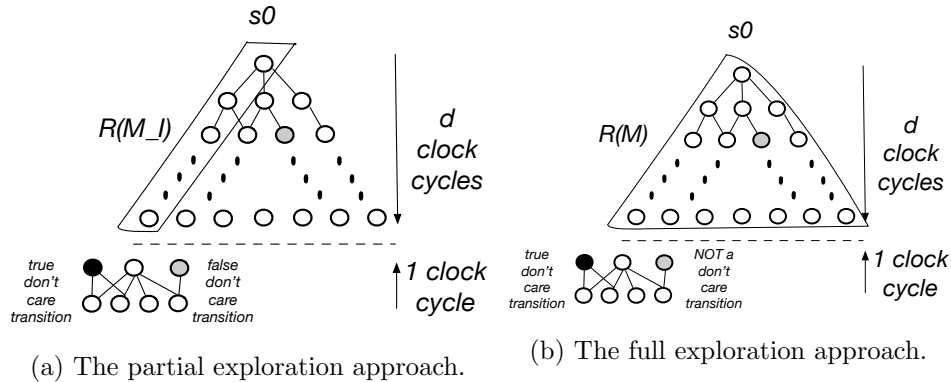


Figure 5: Two approaches for detecting don’t care transitions using symbolic execution. d is the diameter of the analyzed Mealy machine M . I denotes an input sequence. $R(M)$ and $R(M_I)$ denote the set of reachable states in M and in a partition of M w.r.t. the input sequence I , respectively. Black nodes represent unreachable states.

In the second stage, we perform symbolic execution for one clock cycle. *Also, we label both the input variables and the FSM’s state variable as symbolic.* Although symbolic execution is a type of forward analysis, by marking the state variable, e.g., `pcmSq` in Figure 2, as symbolic we are able to simulate the backward analysis, which finds the predecessors of every state. Therefore, this stage is an approximate execution as opposed to the precise execution in the forward stage. This means that it is possible that the source state is an unreachable state, e.g., `pcmSq == 6`. Although an approximate analysis like this may lead to false positives when reasoning about the behavior that the circuit may demonstrate, at the same time, it reveals the don’t care transitions, the main goal of this stage, as a don’t care transition is from an unreachable state to a reachable state. So, in this approximate stage, we use the set of reachable states computed in the forward stage to check whether the source state is an unreachable state and the destination state is a reachable state. Such transitions are identified as don’t care transitions and are reported to the user.

To implement the two stage approach for don’t care transition detection using symbolic execution, we have mainly two options as shown in Figure 5. Figures 5.a and 5.b both show the symbolic execution trees for a Mealy machine under analysis. In these figures, the circles with black color represents the unreachable states and all other states are the reachable ones.

The first option of using symbolic execution is depicted in Figure 5.a, which considers each symbolic execution path as a partition of the Mealy machine M with respect to an input sequence I (see Definition 6) as long as the diameter of M and computes the set of reachable states that have been encountered on that path: $R(M_I)$. However, as indicated by Claim 2, the set of reachable sets observed in a partition may miss some of the reachable states as illustrated by the gray colored state in Figure 5.a. As a result, it is possible to identify some states as unreachable while they are reachable on a different symbolic execution path that exercises a different input sequence. Therefore, with the partial exploration of the reachable states, it is possible to have false positive don’t care transitions. For the FSM in Figure 2, if at each clock cycle on a symbolic execution path the input `inValid` evaluates to false, only ‘`PCM_IDLE`’ would be considered as a reachable state as the FSM state will not change (line 13) and the other 4 reachable states would be incorrectly considered as unreachable.

The second option of using symbolic execution is depicted in Figure 5.b, which computes the set of reachable states by the full exploration of the input space for the Mealy machine M and up to the diameter of M . Unlike the partial approach, this technique can in theory guarantee precision of the set of reachable states. This means that all the reported don’t care transitions would be true positives. However, due to the well-known path explosion problem of symbolic execution, it may not be feasible to explore the full state space.

Symbolic execution engines, such as KLEE, typically implement various path exploration strategies to deal with the path explosion problem. In addition to the classical search algorithms such as Depth-First Search (DFS) and Breadth-First Search (BFS), random and coverage based path exploration strategies exist.

In this paper, we propose and analyze three variations of don’t care transition detection based on the two main approaches and the path exploration algorithms. The three approaches are as follows:

The partial exploration approach This is the approach that is depicted in Figure 5.a and uses a single symbolic execution path to compute the set of reachable states. It also uses the default path exploration strategy of KLEE, which is a combination of random and coverage based.

```

1  always @(posedge clock or negedge reset)
2      begin
3          if (reset) trojan_state <= trojan_idle;
4          else begin
5              case (trojan_state)
6                  trojan_idle: begin
7                      if (pcmSq == 3'd6 || pcmSq == 3'd7)
8                          trojan_state <= trojan_active;
9                      else
10                         trojan_state <= trojan_idle;
11                     end
12                 trojan_active: begin
13                     if (pcmSq == 3'd0)
14                         trojan_state <= trojan_work;
15                     else
16                         trojan_state <= trojan_active;
17                     end
18                 trojan_work: trojan_state <= trojan_work;
19             endcase
20         end
21     end
22     always @(posedge clock or negedge reset)
23         if (reset) trojan_ena <= 1'b0;
24         else if (trojan_state==trojan_work)
25             trojan_ena <= 1'b1;

```

Figure 6: A Trojan that gets triggered upon a don't care transition within the FSM of IMA ADPCM benchmark.

BFS-based exploration This is the approach that is depicted in Figure 5.b and performs a full exploration of the symbolic execution tree in the forward stage using the BFS exploration strategy.

BFS-based exploration with pruning This is a variant of the full exploration approach that is depicted in Figure 5.b. However, we configure the symbolic execution engine to use the BFS exploration strategy with a pruning technique that leverages Claim 1, which implies that if a state has already been explored in BFS then exploring the state at the same or lower layer in the symbolic execution tree (same or higher rank) would not yield finding more reachable states from that state. Therefore, in this approach we kill symbolic execution states with a state of the Mealy machine that has been encountered before.

3.3 Detecting Trojans Triggered by Don't Cares

In this section, we present our overall approach for don't care transition triggered Trojan detection.

Figure 6 shows the Trojan trigger logic that we implemented as an FSM and added to the IMA ADPCM benchmark. The Trojan is initialized to be in the `trojan_idle` state (line 3). When the FSM in Figure 2 reaches one of the states that are normally unreachable (states with values 6 or 7 as shown at line 7), possibly through a physical attack such as voltage glitch, the Trojan FSM transitions to the `trojan_active` state (line 8). However, to trigger the Trojan, the FSM waits to detect transitioning to a reachable state from an unreachable state, i.e., detecting a don't care transition, which is detected at line 13 and at line 14 the Trojan FSM's state is updated to `trojan_work`. Finally, the always block at lines 22-25 sets the `trojan_ena` line to high to denote

```

1  always @ (posedge clock or posedge reset)
2  begin
3      if (reset)
4          begin
5              outPCM <= 4'b0;
6              outValid <= 1'b0;
7          end
8      else if (pcmSq == 'PCM_DONE)
9          begin
10             outPCM <= prePCM;
11             outValid <= 1'b1;
12         end
13     else if (trojan_ena)
14         //trojan payload, stuck at 1 fault
15         outValid <= 1'b1;
16     else
17         outValid <= 1'b0;
18 end

```

Figure 7: The Trojan payload for the IMA ADPCM benchmark.

that the Trojan payload can now be activated.

Figure 7 shows the Trojan payload (lines 13-15), which sets the output line `outValid` to high when it is supposed to be low according to the original design.

Algorithm 2: Detecting Trojans hidden at don't care transitions of a HW Design that is represented by program P .

Input: P : HW Design, $SVar$: FSM State Variable, $Input$: Input Variables, $Output$: Output Variables, d : Diameter

Output: Divergent behavior of the Trojan in P , if any

```

1  ( $RS, RBS$ )  $\leftarrow SymEx(P, \{Init(P)\}, Input, Output, SVar, d, Reach)$ ;
2  ( $Trans, SymStates$ )  $\leftarrow SymEx(P, True, Input \cup \{SVar\}, Output, SVar, 1, States)$ ;
3   $DCT \leftarrow \{(s_1, s_2) \mid s_1 \notin RS \wedge (s_1, s_2) \in Trans\}$ ;
4  if  $DCT = \emptyset$  then
5      print "No don't care transitions and relevant Trojans";
6      return  $\emptyset$ ;
7  end
8   $DBS \leftarrow \emptyset$ ;
9   $Dest \leftarrow \{symst \mid Project(symst, SVar) = s_2 \wedge \exists s_1. (s_1, s_2) \in DCT\}$ ;
10 for each  $s \in Dest$  do
11     ( $RS', RBS'$ )  $\leftarrow SymEx(P, \{s\}, Input, Output, SVar, d, Reach)$ ;
12      $DBS \leftarrow DBS \cup RBS' \setminus RBS$ ;
13 end
14 if  $DBS \neq \emptyset$  then
15     print "Trojan detected";
16 end
17 return  $DBS$ ;

```

Algorithm 2 shows all stages of our Trojan detection approach. In the first phase (line 1), the

algorithm performs the full exploration of the symbolic execution tree for d clock cycles as shown in Figure 5)b to compute the set of reachable states, RS , and the intended set of behaviors, RBS , in terms of a tuple consisting of the source state, s , the destination state, s' , enabling input, I , and the generated output O .

Algorithm 3: Symbolic Execution Algorithm (**SymEx**) as adapted for a HW design.

Input: P : HW Design, $Init$: Initial State(s), $Input$: Input Variables, $Output$: Output Variables, $SVar$: FSM State Variable, N : Number of Clock Cycles, $Type$: Metadata Type

Output: Metadata

```

1  $M$ : Metadata;
2  $M \leftarrow (\{Project(Init, SVar)\}, \emptyset)$ ;
3  $Init.numSteps \leftarrow 0$ ;
4  $Active \leftarrow Init$ ;
5 while  $Active \neq \emptyset$  and  $\exists s \in Active$  s.t.  $s.numSteps < N$  do
6    $symState \leftarrow chooseNext(Active)$ ;
7   if  $symState.numSteps < N$  then
8     Symbolize  $Input$  in  $symState$ ;
9      $succs \leftarrow SymExForOneClockCycle(symState)$ ;
10     $Active \leftarrow Active \setminus \{symState\}$ ;
11    for each  $s \in succs$  s.t.  $s$  not terminated do
12       $s_1 \leftarrow Project(symState, SVar)$ ;
13       $s_2 \leftarrow Project(s, SVar)$ ;
14      if  $Type$  is Reach then
15         $I \leftarrow Project(s, Input)$ ;
16         $O \leftarrow Project(s, Output)$ ;
17         $M.RS \leftarrow M.RS \cup \{s_2\}$ ;
18         $M.RBS \leftarrow M.RBS \cup \{(s_1, s_2, I, O)\}$ ;
19      end
20      if  $Type$  is States then
21         $M.Trans \leftarrow M.Trans \cup \{(s_1, s_2)\}$ ;
22      end
23       $Active \leftarrow Active \cup \{s\}$ ;
24       $s.numSteps \leftarrow symState.numSteps + 1$ ;
25    end
26  end
27 end
28 if  $Type$  is Reach then
29   return  $(M.RS, M.RBS)$ ;
30 end
31 if  $Type$  is States then
32    $M.SymStates \leftarrow Active$ ;
33   return  $(M.Trans, M.SymStates)$ ;
34 end

```

In the second phase (lines 2-7), the algorithm computes the set of don't care transitions, DCT ,

based on the set of reachable states and the transition function. Any transition that starts from an unreachable state and ends at a reachable state is included in *DCT*. If there are no don't care transitions, then the algorithm terminates as there cannot be any Trojans that would be triggered with don't care transitions. Otherwise, the algorithm moves to the third phase (lines 8-13), to identify any divergent behavior that the design can demonstrate once triggered by the don't care transition.

Algorithm 3 presents an abstracted version of the symbolic execution algorithm as adapted to a hardware design, at RTL or gate-level. We assume that P represents a program that simulates the behavior of a hardware design. In our approach, P is generated by Verilator from a given Verilog design. The algorithm gets the set of initial states, the input variables, the output variables, the variable in P that represents the FSM state, the number of clock cycles, and the type of metadata to be computed and returned.

Algorithm 3 keeps track of the explored symbolic execution states in the *Active* set. It associates the number of clock cycles, *numSteps*, initializes it to 0 (line 3), and updates it (line 24) as the design is symbolically executed for one clock cycle each time (line 9).

In Algorithm 3, our major extension to standard symbolic execution is to extract various types of metadata to be used in don't care transition and Trojan detection. One type of metadata, denoted by *Type*, is *Reach*, in which case it computes the set of reachable states RS , and the set of observable behaviors, RBS . It is important to note that in Algorithm 3, the set of initial states is provided as an input and so the notion of reachable is relative to the set of initial states. This is because we instantiate Algorithm 3, in three different ways from Algorithm 2. The first instantiation that performs the forward analysis uses the initial state of the design according to the standard semantics of the RTL design. The second instantiation uses any state, denoted by *True*, as the initial state to perform the 1 clock cycle backward analysis. Finally, in the third instantiation, we use states that have been reached from an unreachable state, as the initial state. However, the symbolic execution state that corresponds to such a state also include any side effect of the Trojan trigger, e.g., the flag that enables the Trojan payload may have been set to true. This is because such symbolic execution states are returned as an output of the second instantiation, which has used the metadata type *State*. So, when this type of metadata type is chosen, Algorithm 3 computes the transition relation in *Trans* and the active set of symbolic execution states in *SymStates*. In most of the metadata computation the FSM state is extracted from the symbolic execution state s with the expression $Project(s, SVar)$, where $SVar$ is the variable that implements the FSM state, e.g., *pcmSq* in Figure 2.

4 Evaluation

We have evaluated the effectiveness of our approach in terms of don't care transition detection (Section 4.1) at RTL (Section 4.1.1) and at gate-level (Section 4.1.2), and in terms of Trojan detection (Section 4.2).

To evaluate our approach, we used benchmarks from *OpenCores* [17] and *Trust-Hub* [22] (except *prep3* and *prep4*, which we got from [20]). These benchmarks are all described at RTL. For each benchmark, the user needs to provide the number of clock cycles for the forward analysis stage and the name of the variable that represents the state in the FSM. Based on these two values a test driver is developed to execute the *eval* function of the top Verilog module with symbolic inputs.

In only two of the benchmarks (AES128 and UART), there are more than one FSMs, e.g. *AES128_1* and *AES128_2* are two different FSMs in AES128. It is obvious that when there are multiple FSMs

Table 1: Summary of Don't Care Transition Detection at RTL (**R**) and at Gate-Level Netlist as Generated by YOSYS (**Y**) and SDC (**S**).

Benchmark	Expl. Method	d	RS			DCT			Dest			Time (min)		
			R	Y	S	R	Y	S	R	Y	S	R	Y	S
prep3_binary	BFS	6	8	8	8	0	0	0	0	0	0	58.52	83.47	15.38
	BFS + Pr.	6	8	8	8	0	0	0	0	0	0	9.13	21.07	3.33
prep4_binary	BFS	8	16	16	16	0	0	0	0	0	0	TO	TO	56.08
	BFS + Pr.	8	16	16	16	0	0	0	0	0	0	20.12	710.17	8.87
AES128_1	BFS	5	5	5	5	3	15	9	3	5	3	16.25	68.53	431.42
	BFS + Pr.	5	5	5	5	3	15	9	3	5	3	4.05	27.52	81.83
AES128_2	BFS	5	4	4	3	0	0	3	0	0	3	13.72	14.35	13.01
	BFS + Pr.	5	4	4	3	0	0	3	0	0	3	2.82	6.3	2.02
AES128_decrypt	BFS	11	11	11	6	55	54	40	11	6	4	16.67	263.52	714.25
	BFS + Pr.	11	11	11	6	55	54	40	11	6	4	4.83	68.41	493.22
IMA ADPCM	BFS	7	6	6	6	2	12	12	1	6	6	6.58	551.55	616.7
	BFS + Pr.	7	6	6	6	2	12	12	1	6	6	0.78	63.43	323.82
XTEA Crypto	BFS	9	15	15	15	241	241	241	1	1	1	13.08	621.05	TO
	BFS + Pr.	9	15	15	15	241	241	241	1	1	1	4.82	390.13	469.37
APB2SPI	BFS	4	3	3	3	3	3	3	3	3	3	12.88	44.47	81.35
	BFS + Pr.	4	3	3	3	3	3	3	3	3	3	1.53	11.08	12.65
UART_1	BFS	5	7	1	2	7	7	12	7	1	2	64.5	73.72	84.48
	BFS + Pr.	5	7	1	2	7	7	12	7	1	2	6.15	10.40	17.75
UART_2	BFS	4	3	2	2	4	4	4	2	2	2	11.58	248.45	27.97
	BFS + Pr.	4	3	2	2	4	4	4	2	2	2	1.18	80.35	12.53
RS232	BFS	3	5	2	4	15	12	12	5	2	3	2.63	53.62	5.46
	BFS + Pr.	3	5	2	4	15	12	12	5	2	3	0.36	3.25	2.81

inside a design, which is quite common in modern circuits, the interactions between them are absolutely important. However, we analyze each FSM of AES128 and UART one at a time to reduce analysis complexity based on the observation that, firstly, since our analysis is performed within the context of the top module and the whole design along with making all inputs to the top module symbolic, interaction between multiple FSMs can be precisely captured while focusing on the states reached for the specific FSM. Secondly, the property we are interested in is whether all reachable states of an FSM can be explored completely and not whether certain combinations of FSM states are reachable. Lastly, our ground truth analysis using the STGs generated by Intel Quartus shows that we were able to precisely detect the reachable states of a particular FSM of a design with multiple FSMs by analyzing a single FSM at a time.

For discussions at RTL, we generated the State Transition Graph (STG) of the FSM in the RTL design under analysis using commercial software *Intel Quartus* to perform ground truth analysis. While our symbolic execution based approach could generate the transitions in the analyzed FSMs with 100% coverage, it could also detect don't care transitions and the Trojans hidden at such transitions efficiently and accurately.

4.1 Detecting Don't Care Transitions

Although our overall approach, as shown in Figure 1, performs don't care transition detection on the gate-level netlist, this detection can still be performed at RTL to help developers harden their designs. Section 4.1.1 and 4.1.2 presents our results on detecting don't care transitions at RTL and gate-level, respectively.

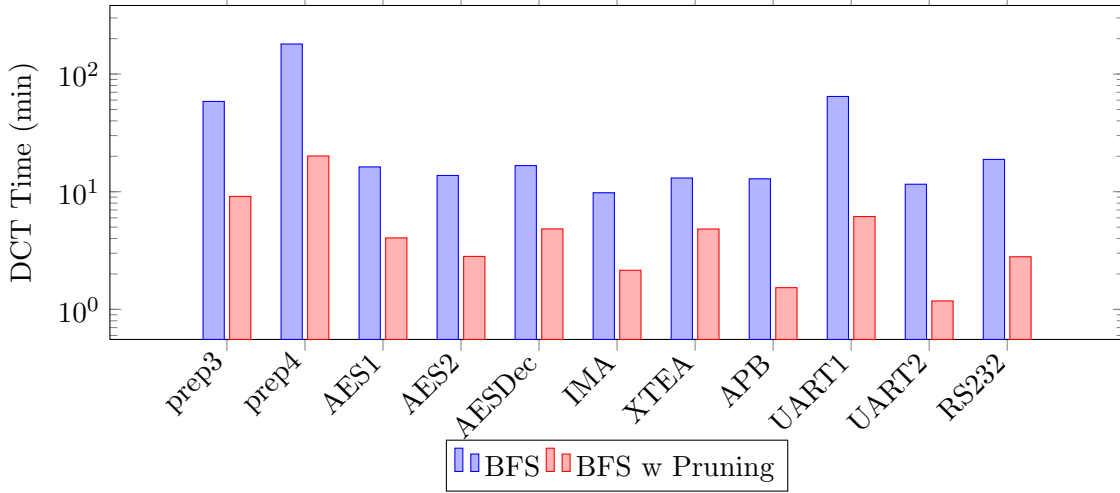
4.1.1 RTL Don't Care Transition Detection

The **Expl. Method** column in Table 1 includes BFS-based full exploration and BFS pruning approaches (denoted by BFS + Pr.). The **d** column represents the number of clock cycles used in the test driver to explore the state space in forward symbolic execution. The next three columns, which represent the size of the set of reachable states, $|RS|$, the number of don't care transitions, $|DCT|$, and the number of unique destinations, $|Dest|$, respectively, are obtained from our method directly without referring to the STG generated by *Intel Quartus*. The seventh column shows the time to find all DCTs in minutes and the timeout was set as three hours.

All the don't care transitions that are detected by full exploration (BFS and BFS with Pruning, denoted by BFS +Pr.) at RTL are true positives. Although not reported in Table 1, we also tested the partial exploration method, which resulted in false positives in most cases (7 out of 11). This was expected based on our discussions in Section 3.2.3. A DCT can be a false positive either due to mislabelling of the source state as unreachable or mislabelling of the destination state as reachable, or both. In the partial exploration approach, the false positives are due to mislabelling of the source state as unreachable. This is because during the partial exploration approach, the states of the FSM may not be fully explored on some symbolic execution paths (or for some input sequences). Therefore, for the rest of the evaluation we use only BFS and BFS with Pruning.

The results in Table 1 also show the scalability and the efficiency of our approach. As more clearly shown in Figure 8, pruning the state space in the forward stage based on previously seen FSM states provides considerable speedup in don't care transition detection time. The average speedup is 6.86 times while maximum speedup is 10.5 times (for `UART1`). Also, for the `prep4.binary` benchmark, BFS without pruning could not report the don't care transition within the timeout of three hours while BFS with pruning reported those in 20.12 minutes.

Figure 8: Comparison of BFS and BFS with Pruning in Don't Care Transition Detection at RTL.



An additional benefit of our approach is the ability to report different cases of the don't care transitions along with the input conditions. For example, Figure 9 presents a constraint that is generated by the symbolic execution engine, which indicates that under the input condition `start_iSec < 2` and `start_iSec ≠ 0` (see the constraints inside the rectangles in Figure 9), `state` could transit from `state < 8` and `state ≠ 0,1,2,3,4` (see the constraints inside rounded rectangles in Figure 9), which means the don't care transition can be from source `state = 5, 6, or 7`, to destination state 0. So, besides reporting don't care transitions, our method can also report the don't care states (unspecified states), state 5, 6 and 7 in this case.

In summary, the analysis time is determined by three aspects. First, the time to detect the don't care transitions become longer as the design gets more complicated. Second, as the number of clock cycles (or `d`) increases, symbolic execution may generate exponentially more paths. Finally, the pruning technique can speedup the detection of don't care transitions by eliminating redundant paths with respect to the FSM states.

4.1.2 Gate-Level Don't Care Transition Detection

Don't care transitions in IPs can be introduced by careless designers, synthesis tools, or both. In this section, two synthesis tools, an open-source software, Yosys Open Synthesis Suite (YOSYS) [26], and a commercial software, Synopsys Design Compiler (SDC) [21], are used to translate RTL designs into the corresponding gate-level netlists. Then we perform our Trojan detection approach on those netlists, and compare these two tools with each other as well as their results with those we obtained from RTL.

YOSYS is an open-source framework for Verilog RTL synthesis. It can take behavioral design description as input and generate gate-level description, either logical gate or physical gate, of the design as output [26]. Thus, in our workflow, gate-level Verilog is first generated by providing a simple script and the remaining steps are the same as that of RTL Verilog (i.e. generate C++ model of gate-level Verilog along with user-provided test harness, compile C++ code, extract LLVM bytecode, and perform symbolic execution).

SDC can automatically synthesize an optimized gate-level circuit based on the design descrip-

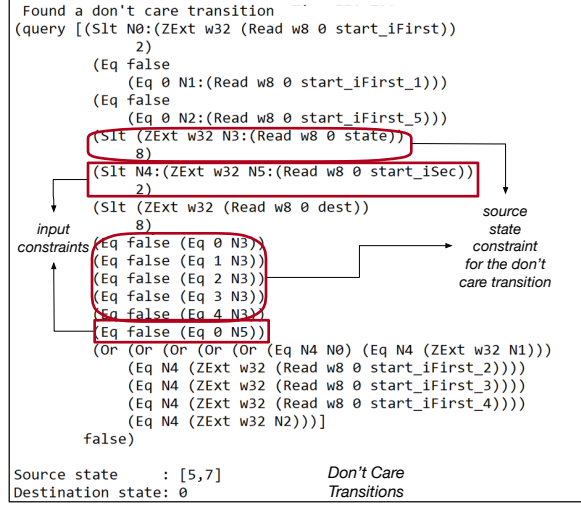


Figure 9: KLEE generated symbolic constraints that describe the inputs enabling the don't care transitions in AES128_1.

tion and design constraints. It can also accept multiple input formats and generate structure Verilog along with multiple performance reports. Workflow in SDC DCT approach is actually same with that of YOSYS DCT approach, except that synthesized gate-level netlist is obtained from *Design.Ultra* with *saed90nm* target library and symbol library.

Table 1 lists the summary of DCT detection at RTL and at gate-level netlist as generated by YOSYS and SDC. As Figure 10 shows for most of the benchmarks the number of DCTs at RTL is same as those at gate-level netlist. However, there are some cases for which the synthesis tool introduces additional DCTs. For example, in two (*AES128_1*, *IMA APDCM*) out of 11 benchmarks, the number of DCTs in the YOSYS-generated gate-level netlist is larger than that of RTL. Similarly, in four (*AES128_1*, *AES128_2*, *IMA APDCM*, *UART_1*) out of 11 benchmarks, the number of DCTs in the SDC generated netlist is larger than that of RTL. On the other hand, in some cases, the synthesis tools may also reduce the number of DCTs. For example, in two (*AES128_decrypt* and *RS232*) out of 11 benchmarks, the number of DCTs in YOSYS-generated and SDC-generated gate-level netlists are smaller than that of RTL. However, for *AES128_decrypt*, SDC has a bigger DCT reduction (15) compared to what is achieved by YOSYS (1). Also, such reductions may be due to the optimization of the FSM as in the case of *RS232*, which is indicated by the reduction in the set of reachable states in the gate-level netlist as shown in Table 1.

To demonstrate effectiveness of performing DCT detection at RTL, run times of each benchmarks regarding RTL, YOSYS- and SDC-generated gate-level netlist are shown by a heatmap in Figure 11. For YOSYS-generated netlist, run times of all gate-level netlist benchmarks increase at most by 81 times (*IMA ADPCM*) compared with that of RTL. Similarly, for all gate-level netlist synthesized by SDC, run times increase at most by 415 times (*IMA ADPCM*) compared with that of RTL.

Additionally, to explain huge runtime increase at gate-level netlist, we report the complexity of each benchmark in software domains, in terms of Software Lines of Code (SW LOC), LLVM instruction count (ICounts), and LLVM branch instruction count (BCounts). As more clearly shown in Fig.12, heatmaps of each complexity criteria are provided. Although it's infeasible to

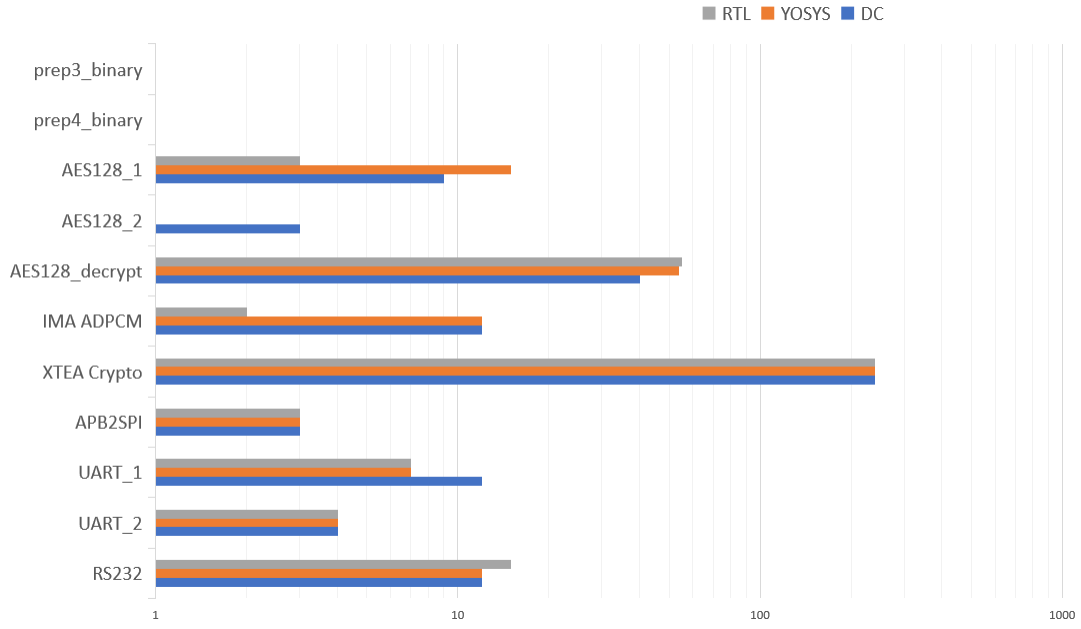


Figure 10: # of DCTs of RTL HDL, YOSYS- and Synopsys Design Compiler-generated gate-level netlist.

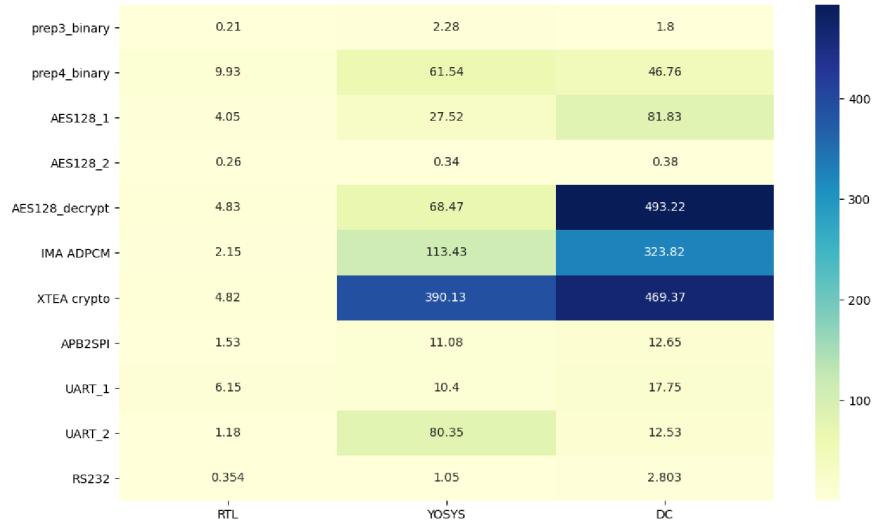


Figure 11: The heat map for the total run time with pruning technique for RTL HDL, YOSYS- and Design Compiler-generated gate-level netlist. All times are reported in minutes, and timeout is 600 minutes.

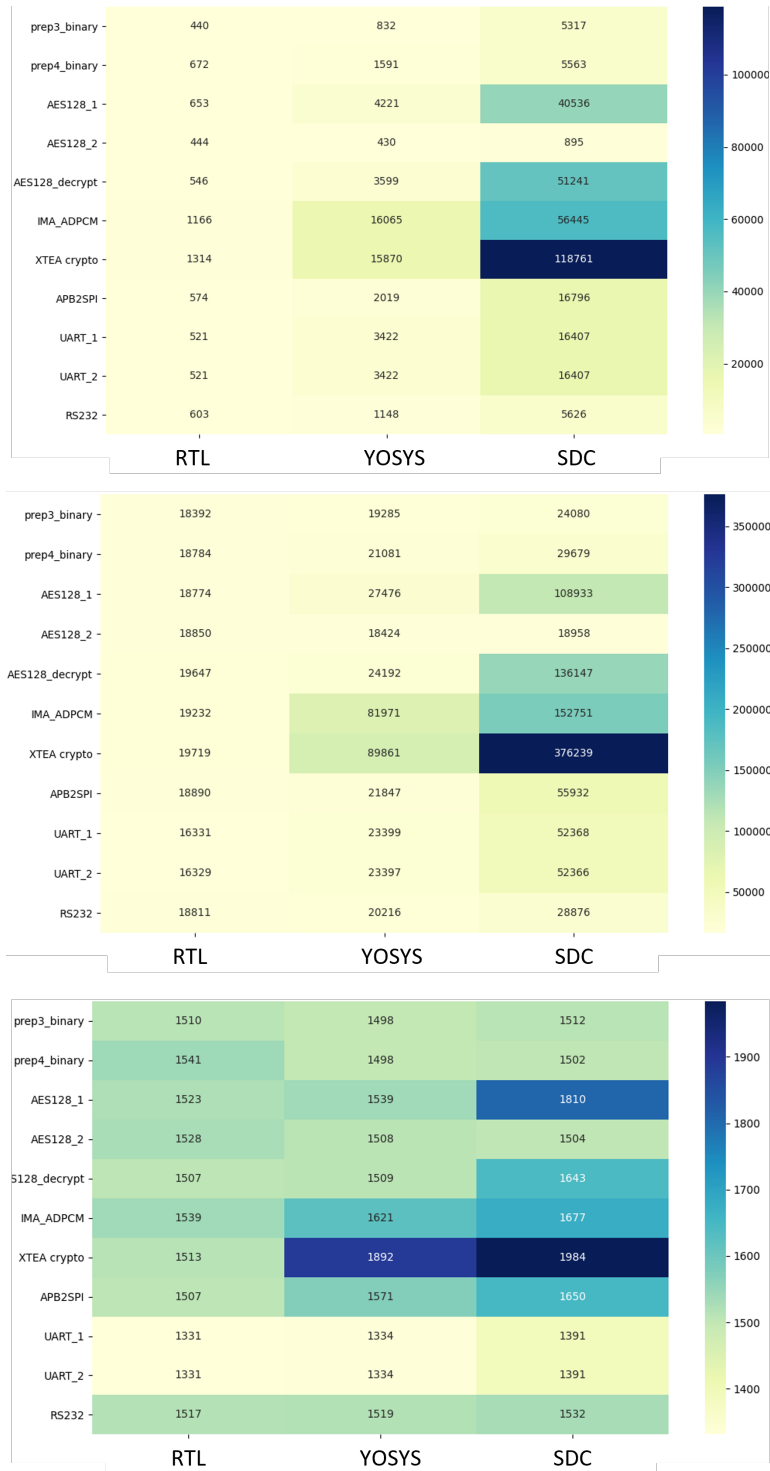


Figure 12: SW LOC, ICounts, and BCounts (from top to bottom respectively) of RTL netlist, YOSYS-generated netlist, and Design Compiler-generated netlist.

determine complexity by a certain criteria, these criteria can be used as indicators to reveal potential complexity. For example, for *IMA_ADPCM*, *XTEA Crypto* in both YOSYS- and SDC-generated netlist, *AES128_decrypt* in SDC-generated netlist, individually each of the three criteria (SW LOC, ICounts, and BCounts) is much larger than that of the other benchmarks, which corresponds to a much larger increase in runtime as shown in Fig.11.

Although it's desirable to perform DCT detection approach at the RTL level for performance reasons, *for soundness DCTs must be detected at the gate-level to account for the DCTs that may be introduced by the synthesis tools.*

4.2 Detecting Trojans Hidden at Don't Care Transitions

We evaluate our Trojan detection approach on two case studies: the RS232-T700 benchmark from **TrustHub** [22] and the IMA ADPCM audio encoding algorithm [25]. Since none of the Trojans in the TrustHub [22] benchmarks use a don't care transition as a trigger, we decided to use existing Trojan payloads from TrustHub and identify RTL designs with FSMs that have don't care transitions so that we could generate new Trojan benchmarks suitable for our approach. So, it turned out that the RS232-T700 benchmark from TrustHub[22], specifically, the transmitter part in RS232-T700, satisfied all our requirements perfectly. Besides, we choose IMA ADPCM benchmark from Opencores [17] for the reason that, both synthesis tools (YOSYS and SDC) could introduce same additional DCTs with the same reachable states, which supports the discussion in Section 4.2.2. We evaluate Trojan detection for the two case studies in Sections 4.2.1 and 4.2.2.

4.2.1 Trojan Detection for IMA ADPCM

In this section, we apply the DCT and Trojan detection method to the encoder part of the IMA ADPCM benchmark. The IMA ADPCM audio compression algorithm belongs to the Adaptive Differential Pulse Code Modulation type algorithms. The algorithm is based on a simple adaptive quantization of the difference between the input and predictor. Each 16-bit input sample is converted to a 4-bit coded information which yields a compression ratio of $\frac{1}{4}$ [25]. We will not go through detailed implementation of the design, instead, we focus on the FSM part, which is shown in Figures 2 and 3.

As summarized in Table 1, for *IMA_ADPCM* benchmark, reachable states at RTL, YOSYS-generated netlist, and SDC-generated netlist are the same (Column $|RS|$). However, # DCTs increases after synthesis (Column $|DCT|$), which means synthesis tools could produce additional DCTs. Trojans that utilize DCTs that are introduced after the synthesis would not be detected if Trojan analysis only checks for DCTs that are detectable at RTL. Therefore, we perform DCT detection at gate-level. However, for this benchmark, since the synthesis preserves the FSM, we can perform Trojan detection, specifically, the divergent output detection stage in Figure 1, at either RTL or gate-level.

Thus, twelve different DCT-triggered Trojan versions of *IMA ADPCM* based on each DCT obtained from analysis at the gate-level netlist are designed as shown in Table 2. It is interesting to note that, in this table, only **ima-1** and **ima-7** represent Trojans triggered by DCTs that only exist at RTL and the remaining ten versions (in blue) indicate Trojans triggered by additional DCTs introduced by the synthesis tool, all activated Trojans will make the output *outValid* stuck at '1'.

As the timing results in Table 2 indicate, Trojan detection at RTL is much faster than the one at gate-level. Specifically, Trojan detection time at gate-level netlist is on average 116.5 times bigger for YOSYS-generated netlist and 353.6 times bigger for SDC-generated netlist than that of Trojan

Table 2: Results on Trojans Triggered by DCTs that Exist at the Synthesised Gate-level Netlist for IMA ADPCM.

Trojan	DCTs	DCT Time (min)		Trojan Time (min)		
		YOSYS	SDC	RTL	YOSYS	SDC
ima-1	T(6→0)	66.61	321.79	1.377	155.52	476.92
ima-2	T(6→1)	67.83	329.43	0.52	159.47	480.33
ima-3	T(6→2)	66.13	318.74	0.538	160.35	485.67
ima-4	T(6→3)	66.56	320.63	0.928	152.93	474.71
ima-5	T(6→4)	67.31	335.41	0.851	158.62	480.43
ima-6	T(6→5)	64.83	328.18	0.819	156.67	477.36
ima-7	T(7→0)	69.15	338.23	1.338	160.56	482.94
ima-8	T(7→1)	66.27	332.38	0.587	153.94	470.83
ima-9	T(7→2)	67.79	337.61	0.598	156.83	475.31
ima-10	T(7→3)	68.71	329.17	0.951	158.20	479.64
ima-11	T(7→4)	67.34	339.56	0.892	156.89	484.13
ima-12	T(7→5)	67.58	332.49	0.871	157.41	487.67

detection at RTL. Also, Trojan detection at gate-level takes much longer for SDC-generated netlists compared to those for YOSYS-generated netlist, which is shown more clearly in Figure 13. This can be explained in terms of the code complexity difference; as shown in Figure 12 SDC-generated netlists are in general more complex than YOSYS-generated netlists.

As shown in Figure 14 and Figure 15, using the hybrid approach of detecting DCTs at gate-level and detecting the Trojans at RTL, we can achieve an average of 3.3X speed-up for YOSYS-generated netlists and an average of 2.46X speed-up for SDC generated netlist.

4.2.2 Trojan Detection for RS232-T700

We modified the RS232-T700 benchmark to generate twelve benchmarks; one for each DCT, and named each one as RS232-T700-N, where N represents the DCT number. Since the synthesis process does not preserve the FSM for this benchmark, as indicated by the columns under $|RS|$ in Table 1, Trojan detection can soundly be performed only at the gate-level for this benchmark.

As the results in Table 3 show, the total analysis time (DCT + Trojan detection) takes at most 15.50 mins and Trojan detection at gate-level takes at most 8.35 mins. This is in contrast with the analysis times for the IMA_ADPCM benchmark, for which gate-level Trojan detection takes at the minimum 152.93 mins. This can be explained with the relative code complexity of these benchmarks: as shown in Figure 12, YOSYS and SDC-generated gate-level netlists for IMA_ADPCM are more complex than those for RS232-T700.

5 Discussion

Our approach has limitations due to several assumptions we make, the type of deviant behavior that we can handle, and the type of benchmarks we used. We assume that we know the diameter of the FSM of interest and the variable (register) that represents the state as our approach expects

Figure 13: Comparison of DCT and Trojan Detection Times on the Synthesized Gate-level Netlists (YOSYS vs SDC generated) for IMA ADPCM. The Trojans are Triggered by DCTs that Exist at the Synthesised Gate-level Netlist.

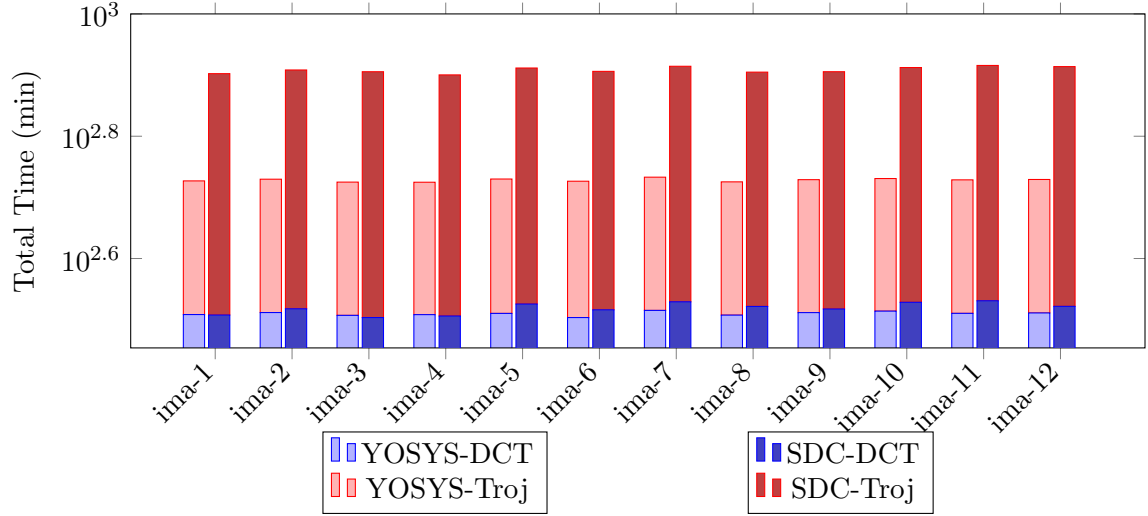
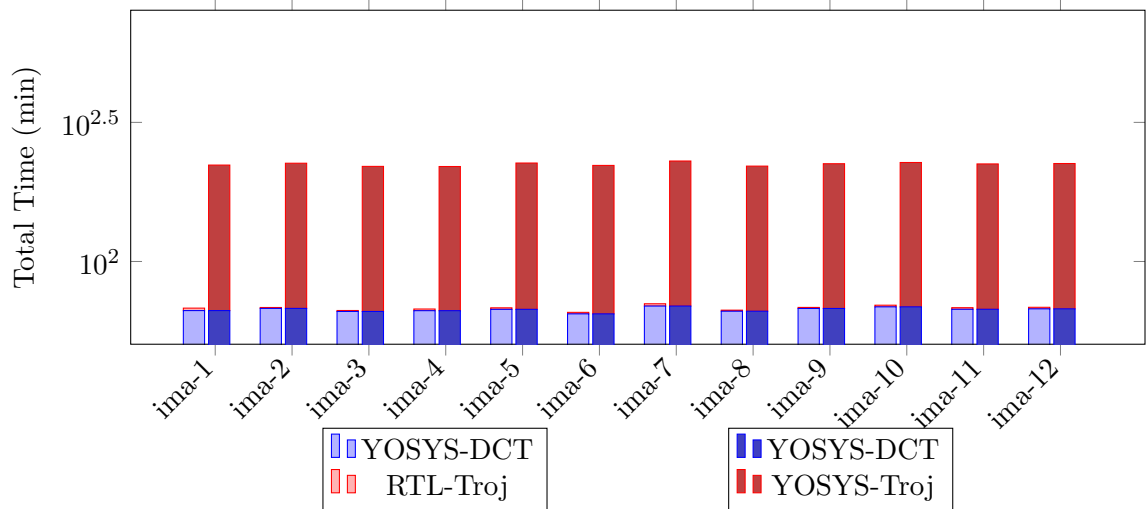
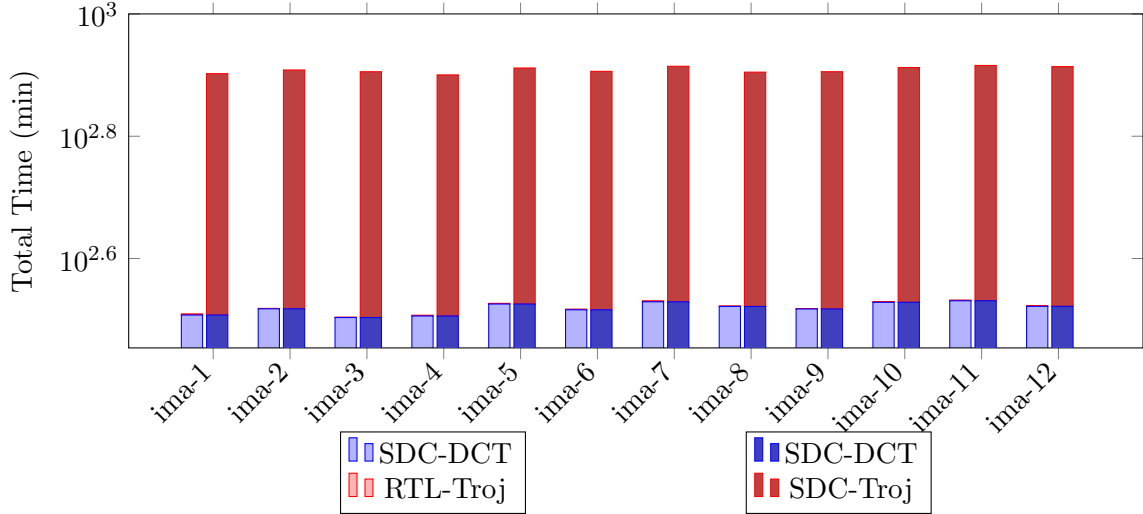


Figure 14: Comparison of YOSYS-Generated Gate-Level Netlist DCT Detection time + RTL Trojan Detection Time vs YOSYS-Generated Gate-Level Netlist DCT + Trojan Detection Time on IMA_ADPCM for Trojans that are Triggered by DCTs that Exist at the Gate-Level Netlist.



these as inputs. Although we were able to easily identify these inputs precisely for the benchmark designs, failing to precisely specify these as input would yield false positives as well as false negatives in Trojan detection. This can happen, for instance, by setting the number of steps to a value that is smaller than the diameter or by not recognizing all registers that represent the states of an FSM, e.g., the combined values of multiple registers represent the state and only a strict subset of these registers are provided as input.

Figure 15: Comparison of SDC-Generated Gate-Level Netlist DCT Detection time + RTL Trojan Detection Time vs SDC-Generated Gate-Level Netlist DCT + Trojan Detection Time on IMA_ADPCM for Trojans that are Triggered by DCTs that Exist at the Gate-Level Netlist.



The second type of limitation is due to detecting deviant behavior in terms of output values. If the Trojan causes other types of side effects such as leaking information through side channels, our approach cannot detect such Trojans. However, our don't care transition detection would still be effective and can guide other approaches that can reason about side channels.

The third type of limitation is due to restricting our analysis to IP-level designs. Although using our pruning techniques we can achieve significant performance improvement, our approach may face the path explosion problem and needs to be improved to scale it to the detection of SOC-level Trojan analysis.

6 Conclusions

We presented a don't care transition and Trojan detection technique that does not require a golden design or a specification. Our approach leverages symbolic execution to achieve high coverage of the reachable and unreachable states in an FSM. Our three stage approach extracts transitions of an FSM and detects don't care transitions, and the Trojans hidden at such transitions. We developed a state space pruning technique and applied our approach to various benchmarks from OpenCores and Trust-hub. Our results show that our approach achieves 100% precision while our pruning technique speeds up detection of the don't care transitions up to 10 times. We show that while don't care transitions must be detected at gate-level, Trojan detection can be performed at RTL provided that the synthesis preserves the FSM structure. In future work, we will investigate scaling our approach to SoC designs and to the detection of Trojans with additional types of payloads.

Table 3: Results on Trojans Triggered by DCTs that Exist at the Synthesized Gate-level Netlist for RS232-T700.

YOSYS-generated netlist					
Trojan	Trigger	d	DCT time (min)	Trojan time (min)	Total time (min)
RS232-T1	T(1→0)	5	8.58	2.18	10.76
RS232-T2	T(1→2)	5	8.32	2.01	10.33
RS232-T3	T(3→0)	5	8.93	2.31	11.24
RS232-T4	T(3→2)	5	9.13	2.44	11.57
RS232-T5	T(4→0)	5	8.53	2.39	10.92
RS232-T6	T(4→2)	5	8.88	2.62	11.50
RS232-T7	T(5→0)	5	9.15	2.61	11.76
RS232-T8	T(5→2)	5	9.02	2.45	11.56
RS232-T9	T(6→0)	5	8.38	2.21	10.59
RS232-T10	T(6→2)	5	8.78	2.37	11.15
RS232-T11	T(7→0)	5	8.34	2.08	10.42
RS232-T12	T(7→2)	5	8.95	2.28	11.23

SDC-generated netlist					
Trojan	Trigger	d	DCT time (min)	Trojan time (min)	Total time (min)
RS232-T1	T(4→0)	5	6.59	7.67	14.26
RS232-T2	T(4→2)	5	6.16	7.13	13.29
RS232-T3	T(4→3)	5	6.85	8.04	14.89
RS232-T4	T(5→0)	5	6.44	7.55	13.99
RS232-T5	T(5→2)	5	7.13	8.29	15.42
RS232-T6	T(5→3)	5	6.73	7.91	14.64
RS232-T7	T(6→0)	5	6.80	7.95	14.75
RS232-T8	T(6→2)	5	6.96	8.09	15.05
RS232-T9	T(6→3)	5	7.15	8.35	15.50
RS232-T10	T(7→0)	5	6.90	7.98	14.88
RS232-T11	T(7→2)	5	6.26	7.33	13.59
RS232-T12	T(7→3)	5	6.94	8.08	15.02

Acknowledgements

This project has been partially funded by NSF Award 2019283. We would like to thank Yier Jin, Xiaolong Guo, and Orlando Arias for the valuable discussions about the synthesis process.

References

- [1] Cristian Cadar, Daniel Dunbar, and Dawson R. Engler. KLEE: unassisted and automatic generation of high-coverage tests for complex systems programs. In Richard Draves and Robbert

- van Renesse, editors, *8th USENIX Symposium on Operating Systems Design and Implementation, OSDI 2008, December 8-10, 2008, San Diego, California, USA, Proceedings*, pages 209–224. USENIX Association, 2008.
- [2] Cristian Cadar and Koushik Sen. Symbolic execution for software testing: three decades later. *Commun. ACM*, 56(2):82–90, 2013.
- [3] Carson Dunbar and Gang Qu. Designing trusted embedded systems from finite state machines. *ACM Transactions on Embedded Computing Systems (TECS)*, 13(5s):1–20, 2014.
- [4] Farimah Farahmandi and Prabhat Mishra. Fsm anomaly detection using formal analysis. In *2017 IEEE International Conference on Computer Design (ICCD)*, pages 313–320. IEEE, 2017.
- [5] Nicole Fern, Shrikant Kulkarni, and Kwang-Ting Tim Cheng. Hardware trojans hidden in rtl don’t cares—automated insertion and prevention methodologies. In *2015 IEEE International Test Conference (ITC)*, pages 1–8. IEEE, 2015.
- [6] Xiaolong Guo, Raj Gautam Dutta, Yier Jin, Farimah Farahmandi, and Prabhat Mishra. Pre-silicon security verification and validation: a formal perspective. In *Proceedings of the 52nd Annual Design Automation Conference, San Francisco, CA, USA, June 7-11, 2015*, pages 145:1–145:6. ACM, 2015.
- [7] Matthew Hicks, Murph Finnicum, Samuel T. King, Milo M. K. Martin, and Jonathan M. Smith. Overcoming an untrusted computing base: Detecting and removing malicious hardware automatically. In *2010 IEEE Symposium on Security and Privacy*, pages 159–172, 2010.
- [8] Tamzidul Hoque, Seetharam Narasimhan, Xinmu Wang, Sanchita Mal-Sarkar, and Swarup Bhunia. Golden-free hardware trojan detection with high sensitivity under process noise. *J. Electron. Test.*, 33(1):107–124, 2017.
- [9] James C. King. Symbolic execution and program testing. *Commun. ACM*, 19(7):385–394, 1976.
- [10] Chris Lattner and Vikram S. Adve. LLVM: A compilation framework for lifelong program analysis & transformation. In *2nd IEEE / ACM International Symposium on Code Generation and Optimization (CGO 2004), 20-24 March 2004, San Jose, CA, USA*, pages 75–88. IEEE Computer Society, 2004.
- [11] Yu Liu, Ke Huang, and Yiorgos Makris. Hardware trojan detection through golden chip-free statistical side-channel fingerprinting. In *Proceedings of the 51st Annual Design Automation Conference, DAC ’14*, page 1–6, 2014.
- [12] LLVM Language Reference Manual. "<https://llvm.org/docs/LangRef.html>".
- [13] Eric Love, Yier Jin, and Yiorgos Makris. Proof-carrying hardware intellectual property: A pathway to trusted module acquisition. *IEEE Transactions on Information Forensics and Security*, 7(1):25–40, 2012.
- [14] Travis Meade, Jason Portillo, Shaojie Zhang, and Yier Jin. Neta: when ip fails, secrets leak. In *Proceedings of the 24th Asia and South Pacific Design Automation Conference*, pages 90–95, 2019.

- [15] Adib Nahiyani, Kan Xiao, Kun Yang, Yeir Jin, Domenic Forte, and Mark Tehranipoor. Avfsm: a framework for identifying and mitigating vulnerabilities in fsm. In *Proceedings of the 53rd Annual Design Automation Conference*, pages 1–6, 2016.
- [16] Seetharam Narasimhan, Xinmu Wang, Dongdong Du, Rajat Subhra Chakraborty, and Swarup Bhunia. Tesr: A robust temporal self-referencing approach for hardware trojan detection. In *HOST 2011, Proceedings of the 2011 IEEE International Symposium on Hardware-Oriented Security and Trust (HOST), 5-6 June 2011, San Diego, California, USA*, pages 71–74. IEEE Computer Society, 2011.
- [17] OpenCores. <https://opencores.org/>.
- [18] Jeyavijayan Rajendran, Vivekananda Vedula, and Ramesh Karri. Detecting malicious modifications of data in third-party intellectual property cores. In *2015 52nd ACM/EDAC/IEEE Design Automation Conference (DAC)*, 2015.
- [19] Michael Rathmair, Florian Schupfer, and Christian Krieg. Applied formal methods for hardware trojan detection. In *2014 IEEE International Symposium on Circuits and Systems (IS-CAS)*, 2014.
- [20] Steve Golson. State machine design techniques for Verilog and VHDL. https://trilobyte.com/pdf/golson_snug94.pdf. Last accessed May 1st, 2021.
- [21] Synopsys. <https://www.synopsys.com/implementation-and-signoff/rtl-synthesis-test/design-compiler-graphical.html>.
- [22] TrustHub. <https://www.trust-hub.org/#/home>.
- [23] VERILATOR. <https://www.veripool.org/verilator/>. Last accessed May 1st, 2021.
- [24] Adam Waksman, Matthew Suozzo, and Simha Sethumadhavan. Fanci: Identification of stealthy malicious logic using boolean functional analysis. In *Proceedings of the 2013 ACM SIGSAC Conference on Computer and Communications Security, CCS '13*, page 697–708, 2013.
- [25] Wiki. <https://wiki.multimedia.cx/index.php>.
- [26] Clifford Wolf. <http://www.clifford.at/yosys/about.html>.
- [27] Kan Xiao, Domenic Forte, Yeir Jin, Ramesh Karri, Swarup Bhunia, and Mark Mohammad Tehranipoor. Hardware trojans: Lessons learned after one decade of research. *ACM Trans. Design Autom. Electr. Syst.*, 22(1):6:1–6:23, 2016.
- [28] Hao Xue and Saiyu Ren. Self-reference-based hardware trojan detection. *IEEE Transactions on Semiconductor Manufacturing*, 31(1):2–11, 2018.
- [29] Mingfu Xue, Rongzhen Bian, Weiqiang Liu, and Jian Wang. Defeating untrustworthy testing parties: A novel hybrid clustering ensemble based golden models-free hardware trojan detection method. *IEEE Access*, 7:5124–5140, 2019.
- [30] Ghobad Zarrinchian and Morteza Saheb Zamani. Latch-based structure: A high resolution and self-reference technique for hardware trojan detection. *IEEE Transactions on Computers*, 66(1):100–113, 2017.

- [31] Jie Zhang, Feng Yuan, Linxiao Wei, Yannan Liu, and Qiang Xu. Veritrust: Verification for hardware trust. *IEEE Transactions on Computer-Aided Design of Integrated Circuits and Systems*, 34(7):1148–1161, 2015.
- [32] Rui Zhang, Calvin Deutschbein, Peng Huang, and Cynthia Sturton. End-to-end automated exploit generation for validating the security of processor designs. In *51st Annual IEEE/ACM International Symposium on Microarchitecture, MICRO 2018, Fukuoka, Japan, October 20-24, 2018*, pages 815–827. IEEE Computer Society, 2018.
- [33] Xuehui Zhang and Mohammad Tehranipoor. Case study: Detecting hardware trojans in third-party digital IP cores. In *HOST 2011, Proceedings of the 2011 IEEE International Symposium on Hardware-Oriented Security and Trust (HOST), 5-6 June 2011, San Diego, California, USA*, pages 67–70. IEEE Computer Society, 2011.
- [34] Xuehui Zhang, Kan Xiao, Mohammad Tehranipoor, Jeyavijayan Rajendran, and Ramesh Karri. A study on the effectiveness of trojan detection techniques using a red team blue team approach. In *31st IEEE VLSI Test Symposium, VTS 2013, Berkeley, CA, USA, April 29 - May 2, 2013*, pages 1–3. IEEE Computer Society, 2013.